A Recuperative Heat Exchanger for Space-Borne Turbo-Brayton Cryocoolers

R. W. Hill, M. G. Izenson, W. B. Chen and M. V. Zagarola

Creare Incorporated
Hanover, NH USA 03755

ABSTRACT

The recuperative heat exchanger in turbo-Brayton cryocoolers is often the largest and heaviest cryocooler component, and its performance has a direct impact on the available cooling, and consequently, the cycle efficiency. The design of this component is also quite challenging as structural goals associated with vibration loads are often in conflict with thermal goals for low axial conduction. Creare has developed the only space qualified recuperator for turbo-Brayton cryocoolers. This recuperator is currently installed on the Hubble Space Telescope as part of the NICMOS cryocooler (NCC), which has operated on-orbit for over 4 years without degradation. The NCC recuperator technology has demonstrated extremely high thermal performance and structural robustness. The recuperator went through extensive structural tests prior to installation including two random vibration tests, two shuttle launches, and one shuttle landing. Under support from NASA and MDA, Creare has been developing the next generation recuperator technology. The advanced recuperator technology is based on silicon slotted plates as the heat transfer elements to provide high stream-to-stream conductance and low mass. An innovative core construction minimizes axial conduction and supports the core against launch vibrations. The resulting recuperator is predicted to provide the same high thermal performance as the NCC recuperator for a fraction of the size and weight. This paper reviews the recuperator design, and the results of vibration and thermal tests.

INTRODUCTION

Future space missions for the Department of Defense (DoD) and NASA may require mechanical cryocoolers for cooling infrared detectors. These cryocoolers will need to be efficient, lightweight and highly reliable to meet mission objectives. Typical cooling loads range from hundreds of milliwatts at 10 K to several watts at 35 K up to approximately 10 watts at 70 K, depending on the specific focal plane technology and size, with additional loads at higher temperatures for cooling optics and for shielding. The dual cooling loads are usually absorbed using a two-stage cryocooler, which has benefits in terms of size and mass relative to two single-stage coolers. In addition, low exported vibration is a key requirement for missions where precise pointing accuracy is required. Low vibration is difficult to achieve with Stirling-class cryocooler technologies which utilize reciprocating compressors (and expanders in some cases). Vibration cancellation techniques have been demonstrated to reduce exported vibration to below 100 mN,[1] but this value is still unacceptable for some missions. Turbo-Brayton cryocoolers

Cryocoolers 14, edited by S.D. Miller and R.G. Ross, Jr.

offer a very low vibration alternative. These cryocoolers utilize gas-bearing turbomachines with miniature precisely balanced rotors to compress and expand the working gas. The result is almost imperceptible exported vibration without the need for vibration cancellation. However, turbo-Brayton cryocoolers are generally larger and heavier than their Stirling-class counterparts due primarily to current recuperator technology.

A single turbo-Brayton cooler has been space flight qualified and implemented in a space application. The NICMOS Cryogenic Cooler (NCC) is a single-stage turbo-Brayton cryocooler that was installed on the Hubble Space Telescope (HST) in early 2002.[2] This cryocooler provides 7 W of cooling at 70 K to the NICMOS instrument, replacing the solid nitrogen cryogen that had prematurely depleted. The NCC returned the instrument to operation within one month of installation and has maintained the instrument at the optimum temperature for over 4 years (as of May 2006). The retrofit of NICMOS instrument with a turbo-Brayton cryocooler was an unqualified success, meeting all requirements. On orbit operation has shown that emitted vibrations and temperature stability of the cryocooler are within the restrictive requirements of the application. This cooler demonstrated the features and advantages of turbo-Brayton cryocoolers for space applications. Other programs have successfully demonstrated the technology at temperatures of 35 K[3] and at even lower temperatures.[4] Advanced development programs are focused on components that are lighter, smaller and have higher performance. This paper reviews our progress on developing the next-generation recuperator for turbo-Brayton cryocoolers.

RECUPERATORS FOR TURBO-BRAYTON CRYOCOOLERS

The impact of recuperator performance on the performance of a single-stage turbo-Brayton cryocooler is shown in Figure 1 for three cryocooler designs optimized for different load temperatures. Here, the cryocooler performance is represented as a fraction of the Carnot cycle performance, and the recuperator loss is represented as a fraction of the turbine refrigeration. For a calorically perfect gas, the recuperator loss ($\dot{Q}_{recuperator}$) is given by:

$$\dot{Q}_{recuperator} = \dot{m} C_p I \left(T_{hpi} - T_{lpi} \right) \tag{1}$$

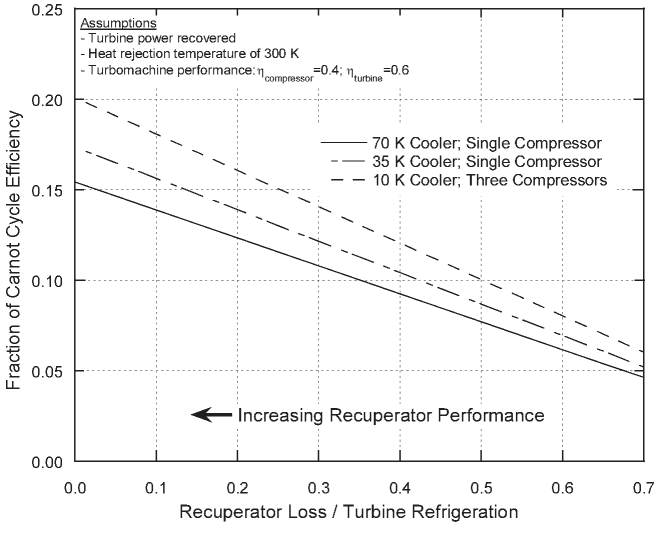

Figure 1. Impact of Recuperator Performance on Single-Stage Turbo-Brayton Cryocooler Performance

where $\dot{m}$ is the mass flow rate, C_p is the specific heat, I is the thermal ineffectiveness (=1-effectiveness), and $T_{hpi}–T_{lpi}$ is the difference between the high and low pressure inlet gas temperatures. In addition to thermal ineffectiveness, low cycle pressure drop is critical to cycle performance as it allows the full pressure ratio produced by the compressor to be expanded across the turbine. Consequently, a high performance recuperator is characterized by low thermal ineffectiveness and low pressure drop.

For a cooler with ideal recuperation, the recuperator loss is equal to zero ($I = 0$), and the net refrigeration is equal to the turbine refrigeration. For space applications, the high cryocooler performance associated with low recuperator losses must be traded with mass, packaging and parasitic considerations associated with a potentially larger recuperator. Performance levels of 12-17% of the Carnot cycle performance are possible with turbo-Brayton cryocoolers if recuperator performance penalties are maintained to about 20% of the turbine refrigeration. These cryocooler performance levels are considerably higher than current space-borne cryocoolers of any technology class, which may achieve up to ~12% of the Carnot cycle performance (performance is defined here on DC input power to the compressor). Even higher performance levels can be attained with turbo-Brayton cryocoolers in two-stage configurations and with higher performance turbomachines. These factors will not be reviewed in this paper.

The current state-of-the-art recuperator for space systems is Creare's Slotted-Plate Heat Exchanger (SPHX). This recuperator is comprised of a stack of copper plates containing concentric rings of slotted flow passages. The precision slots are formed using an automated Electric-Discharge Machining (EDM) process. The recuperator core consists of plates that are separated by low-conductivity stainless steel spacers brazed between the concentric rings of slots. The core is placed inside a stainless steel shell (i.e., tube), and the shell is welded to headers to form an all-metal hermetic unit. The total number of plates in the recuperator is selected based on a trade between input power and cryocooler size/mass. This type of recuperator was space qualified during the NCC program, has been tested at temperatures from 300 K to 5 K, and has demonstrated a thermal effectiveness of 0.997 with low pressure drop. The NCC recuperator loss is estimated to be 30-35% of the turbine refrigeration. Despite the excellent performance and high level of maturity of the copper-stainless steel (Cu-SS) SPHX, many future space missions will require lighter and smaller recuperators that can still attain high performance.

A candidate recuperator for future turbo-Brayton cryocoolers is the Silicon Micro-Machined Recuperator (SMR). The key elements of the technology are silicon slotted plates and non-conductive spacers. The slotted plates are manufactured from single-crystal silicon which has very high thermal conductivity particularly at low temperatures, and the spacers are manufactured from a material that has extremely low thermal conductivity at all temperatures. The slots in the plates are made using a precision photo-etching technique that accurately produces thousands of high aspect ratio slots in a single plate. The micro-slots provide high heat transfer coefficients and large heat transfer area in a small volume. The combination of lightweight materials with excellent thermal properties, and the use of precision photo-etching techniques enable recuperators to be produced that are smaller, lighter and have higher performance than the current state of the art.

SILICON RECUPERATOR DESIGN

Figure 2 illustrates the SMR concept. This particular recuperator has been optimized for the cold-stage of a two-stage 35 K/85 K cryocooler. Each of the 115 slotted plates is made from a single-crystal silicon wafer. Thousands of slots are etched through the thickness of the wafer and arranged in annular rows. A photograph of a silicon slotted plate is shown in Figure 3. The inner rows carry the flow of the high-pressure stream and the outer rows carry the low-pressure flow. The spacers are placed between silicon plates to limit the conductive heat transfer along

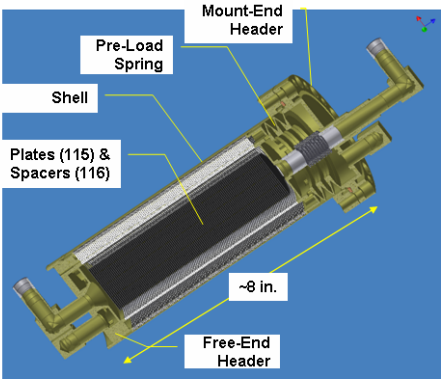

Figure 2. Silicon Micro-Machined Recuperator

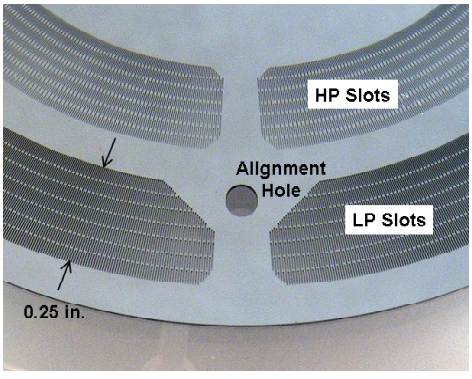

Figure 3. Silicon Slotted Plate

the recuperator axis, and are configured in a geometry that separates the high and low pressure gas streams. The plates and spacers are stacked to form the core. Titanium alloy headers are added to the core and a titanium alloy shell is placed over the assembly. One of the headers includes a preload spring that maintains the plates and spacers in compression to prevent-cross-stream leakage. During assembly the core is loaded with a prescribed force that compresses the preload spring. The shell is welded to the headers to form a hermetic, all-metal pressure boundary.

A comparison between recuperators based on Cu-SS SPHX and advanced SMR technology is given in Table 1. Both recuperators were optimized for operating conditions consistent with the cold recuperator in a two-stage 35 K/85 K turbo-Brayton cryocooler. For the same performance, the SMR is smaller and lighter than the Cu-SS SPHX. Of particular significance, the core of the SMR is ¼ the mass of a Cu-SS SPHX core providing the same performance. This characteristic will allow the thermal performance of the SMR to be higher than the Cu-SS SPHX with a modest increase in SMR mass.

Table 1. Recuperator Technology Comparison

	Cu-SS SPHX	SMR
Design Conditions		
Mass Flow Rate	1 g/s of Ne	1 g/s of Ne
HP Inlet Temperature	85 K	85 K
LP Inlet Temperature	35 K	35 K
HP Inlet Pressure	3.2 atm	3.2 atm
LP Inlet Pressure	2.0 atm	2.0 atm
Predicted Performance		
Thermal Ineffectiveness	0.012	0.012
Fractional Pressure Drop	< 0.3%	< 0.3%
Design		
Total Mass / Core Mass	4.7 kg / 4.1 kg	1.3 kg / 0.36 kg
Total Length / Core Length	17 in. / 14 in.	8.2 in. / 5.8 in.
Shell Diameter	3.5 in.	2.9 in.
Number of Plates	225	115

SILICON RECUPERATOR TESTING

Two test SMRs were recently built on a project funded by the Missile Defense Agency. The first test recuperator is a vibration test unit that has the same core construction as the recuperator shown in Figure 2, but utilized 60 silicon plates, most of which are without slots to reduce fabrication costs. This recuperator was developed to provide an initial indication of the survivability of the basic design during space launch. The vibration tests are described below. The second test recuperator is a thermal test unit that is identical to the recuperator shown in Figure 2, but utilized 78 slotted silicon plates. The thermal unit was tested in a cryogenic test loop at cold-end temperatures down to 80 K and warm-end temperatures of 130 K to 170 K. The thermal tests are described below. Both units were subjected to and passed a proof pressure test at 1.5x the maximum design pressure (~3x the nominal operating pressure), a cross-stream leakage test and an external leakage test prior to vibration and thermal tests.

In addition to the test SMRs, a subscale core was built on the same project to assess the integrity of internal seals at cryogenic temperatures and to determine the appropriate sealing pressure to be applied by the pre-load spring. The primary parameter of interest during these tests was the cross-stream leakage, which is a cycle performance penalty as it represents flow that required power to be compressed but did not produce useful refrigeration in the expansion turbine. The core sealing tests are also described below.

Core Sealing Tests

The core sealing tests included temperature cycle tests between 300 K and 77 K, and sealing tests at temperatures down to 10 K. The performance goal was a cross-stream leakage value of less than 1% of the cycle flow rate when scaled to a full-scale recuperator. The subscale core consisted of 3 silicon plates and 4 spacers. The core was placed in compression using an adjustable plunger and load cell. In this manner, the compression load could be varied and the impact on seal performance quantified. The leakage was quantified by monitoring the pressure change of a helium filled reservoir over time. Because of the extremely low leakage rates, test durations were typically several hours or more. The core was tested in a nominally isothermal condition. The core temperature was monitored using a thermocouple or platinum resistance thermometer, and the temperature was set by suspending the core over liquid nitrogen or liquid helium, both depending on the test temperature.

Initial tests to determine an acceptable sealing pressure were performed at 77 K. The subscale core was then subjected to 20 temperature cycles between 300 K and 77 K. No change in leakage was observed during and after the cycles. As a final acceptance test, the subscale core was leak tested at temperatures down to 10 K. Leakage rates were extremely low and acceptable for even a modest sealing load and temperatures down to 10 K. Leakage measurements at temperatures below 10 K were not made due to limitations in the test set-up.

Vibration Tests

A test recuperator was subjected to random vibration tests and tap tests in directions lateral to and parallel to the recuperator axis. The test set-up for the lateral tests is shown in Figure 4. The recuperator was mounted in a cantilevered configuration through a fixture to a Labworks Model ET-140 Shaker. Different fixtures were used for the lateral and axial tests. A response accelerometer was attached to the free-end recuperator header and a control accelerometer was attached to the shaker. Tap tests were performed using an impact hammer. The random vibration tests were planned to be performed at three incremental levels up to the qualification-level power spectrum provided in GEVS-SE published by NASA/GSFC (14.1 G_{rms}; 0.16 G^2/Hz peak).[5] Limitation with the test set-up and shaker reduced the maximum acceleration levels to somewhat below the qualification levels. The maximum acceleration level tested at in the lateral direction was 12.5 G_{rms}, and the maximum acceleration tested at in the axial direction was 7.9 G_{rms}. The measured input spectrum for the lateral random vibration test is shown in Figure 5.

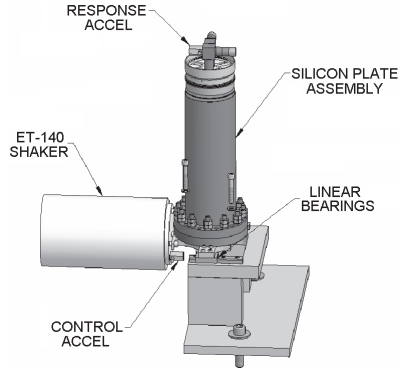

Figure 4. Test Set-Up for the Lateral Vibration Tests

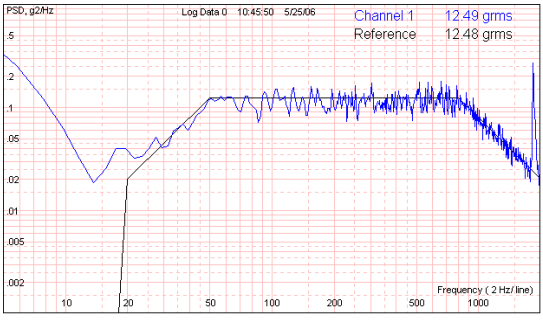

Figure 5. Input Spectrum for the Lateral Random Vibration Tests

An external leakage test and a cross-stream leakage test were performed before, after and at intervals between the random vibration tests to identify if any failures had occurred. The external leak rate was better than 0.5×10^{-9} std cc He/sec for all leak tests as measured using a calibrated helium mass spectrometer. The cross-stream leakage rate was undetectable when pressurizing the high pressure side with helium and measuring the leak down rate over a 3 hr period using a gage with 0.1 psi resolution.

Thermal Performance Tests

The thermal performance tests were conducted in a reconfigured single-stage turbo-Brayton cryocooler that was previously demonstrated at temperatures down to 30 K.[3] The test SMR was plumbed in series at the cold end of the existing 300-plate Cu-SS slotted plate recuperator. The turboalternator was removed and replaced with a liquid-nitrogen cooled heat exchanger. This approach limited the minimum test temperature to ~80 K but dramatically reduced the test time and costs. The SMR was insulated using 10 layers of Multi-Layer Insulation (MLI) and was tested in a vacuum of better than 10^{-5} torr. Individual MLI layers were separated with polyester scrim. The radiative parasitics and axial conduction within the MLI were calculated and determined to be small (radiative parasitic of 60 mW; axial conduction of 4 mW). A photograph of the cold end prior to lowering the bell-jar is shown in Figure 6.

The performance parameters of interest for the recuperator were the thermal ineffectiveness (= 1 – effectiveness) and the pressure drop. The pressure drop is extremely low by design but was not characterized in this test. The key measurements were the inlet and outlet temperatures to and from the SMR, and the mass flow rate. These temperatures were measured using calibrated Platinum Resistance Thermometers (PRTs) fed to a Lakeshore Model 218S Temperature Indicator. Two PRTs were installed at each location. The worst-case difference between redundant temperature sensors was 200 mK which is nominally consistent with the overlap of the 2σ-uncertainty bands of the measurements (± 90 mK). The average value was used for all performance calculations. The mass flow rate was measured using a venturi meter with an estimated uncertainty of ± 3%. The test loop schematic is shown in Figure 7.

The test plan included tests over a broad range of flow rates and at different pressure ratios. Each pressure ratio and mass flow rate was set by adjusting both the compressor speed and a throttling valve attached to a liquid nitrogen heat exchanger. The tests at different pressure ratios were intended to determine if there was any detectable cross-stream leakage.

The range of mass flow rates was selected to characterize the relative importance of axial conduction and stream-to-stream heat transfer. To first order, the performance of a balanced counter-flow recuperator with axial conduction and negligible parasitics is given by:

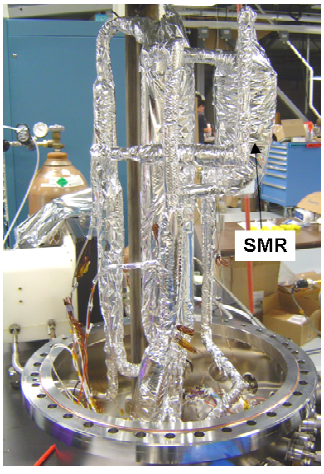

Figure 6. Cold End of Test Loop

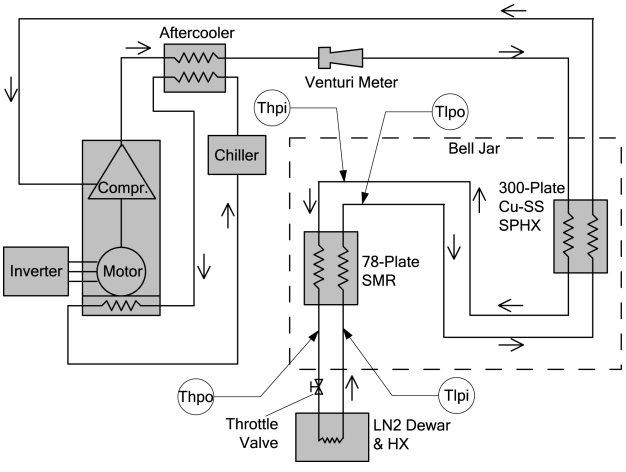

Figure 7. Test Loop Schematic

$$I = \frac{T_{hpi} - T_{lpo}}{T_{hpi} - T_{lpi}} = \frac{T_{hpo} - T_{lpi}}{T_{hpi} - T_{lpi}} = \frac{C}{UA_s} + \frac{1}{CR_a} \tag{2}$$

where C is the heat capacity rate ($\dot{m}C_p$), U is the overall heat transfer coefficient between the gas streams, A_s is the heat transfer surface area, R_a is the axial resistance of the heat exchanger, and T is the fluid temperature at the inlet and outlet to the high and low pressure streams.[6] The predicted design point of the thermal test unit is at the minimum ineffectiveness, which corresponds to a heat capacity ratio of 1 W/K (1 g/s of neon). The test matrix included test points from 50% to 200% of the design flow rate.

The thermal test results are shown in Figure 8. Here we plot the ineffectiveness as a function of the heat conductance rate for the measured data and predictions. The ineffectiveness measurements are based on the average of the cold end and warm end temperature differences as shown in Equation 2, which agreed to within 0.006. Error bars are represented on Figure 8 as a random uncertainty but most likely include systematic errors associated with parasitics, thermal transients, and implementation of the temperature sensors. The measurements at heat conductance rates of 1 W/K and greater were all taken at two different pressure ratios (~1.15 and 1.75). At each conductance value, the ineffectiveness at the two pressure ratios is nearly identical indicating that the cross-stream leakage is negligible.

The ineffectiveness of the recuperator is approximately double the predictions at the design point. Two possible causes for this behavior were considered that could explain the data. The first cause is an inaccuracy in our performance model for predicting UA_s and R_a values. The performance model has been used to predict the ineffectiveness of Cu-SS slotted plate recuperators to better than ± 10% at ineffectiveness values as low as 0.003. A sensitivity analysis was performed with our performance model to determine whether the accuracy of the material properties or geometric inputs for the SMR could explain the performance shortfall. The sensitivity analysis indicates that a modeling inaccuracy of this magnitude is unlikely.

The second cause considered is an internal leak which allowed the low pressure flow to bypass the core. The bypass flow would rejoin the main flow in the warm-end header at a location upstream of the temperature measurements for the low pressure outlet flow. A low pressure bypass flow would effectively unbalance the recuperator core, limiting the minimum

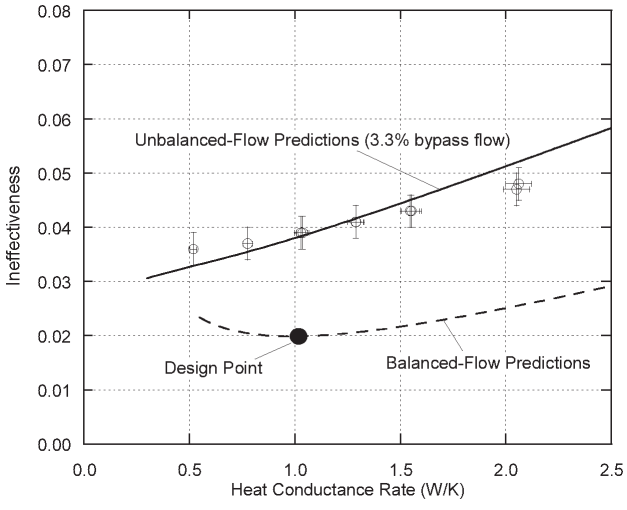

Figure 8. Thermal Performance Test Data

achievable ineffectiveness. A simple model was constructed to predict this behavior. These predictions are shown in Figure 8 for a fixed bypass of 3.3% of the main flow. The agreement between the unbalanced-flow model and test data is good. The correspondence is excellent when the leakage is varied from 3.2% to 3.9% with increasing heat conductance rate from 0.5 W/K to 2 W/K. The recuperator design was reviewed in light of these results and a potential bypass leak path was identified. The bypass leak could be readily addressed in the thermal test recuperator and future designs.

In summary, the thermal performance was less than predicted though it was still excellent. In terms of recuperator design, if the cause of the performance shortfall is the bypass leak mentioned above, then the recuperator technology comparison given in Table 1 is valid, and a 70% reduction in recuperator mass will be realized by replacing the current state of the art with the SMR. If the cause is inaccurate modeling of the UA_s and R_a values (considered to be highly unlikely), then the core size will need to be increased to achieve the desired effectiveness. The larger core increases the SMR mass given in Table 1 to approximately 1.8 kg. Nevertheless, a reduction in recuperator mass of greater than 60% will be realized by replacing the current state-of-the-art recuperator with the SMR.

CONCLUSIONS

A new recuperative heat exchanger for turbo-Brayton cryocoolers has been designed, built, and tested. This new heat exchanger relies on silicon micromachining technology and lightweight materials to significantly reduce the size and weight of the recuperator, and to increase thermal performance relative to the current state-of-the-art recuperator. The recuperator technology is applicable at temperatures of 10 K and possibly lower. Future turbo-Brayton cryocoolers incorporating this recuperator will be lighter, more compact and will require less input power.

ACKNOWLEDGMENT

The support and guidance of the Missile Defense Agency, the Air Force Research Laboratory, and NASA are gratefully acknowledged.

REFERENCES

1. Kirkconnell, C.S., Zagarola, M.V., and Russo, J.T., "Hybrid Stirling/Reverse Brayton and Multi-Stage Brayton Cryocoolers for Space Applications," *Adv. in Cryogenic Engineering*, Vol. 51B, Amer. Institute of Physics, Melville, NY (2006), pp. 1489-1496.
2. Swift, W.L., Cheng, E., Zagarola, M.V., and Dolan, F.X., "On-Orbit Operating Experience with the NICMOS Cryocooler—First Year," *Proceedings of the TDW 2003—International Workshop on Thermal Detectors for Space Based Planetary, Solar, & Earth Science Applications*, Adelphi, MD (June 2003), pp. 19-20.
3. Zagarola, M.V., Dietz, A.J., Swift, W.L., and Davis, T.M., "35 K Turbo-Brayton Cryocooler Technology," *Adv. in Cryogenic Engineering*, Vol. 49B, Amer. Institute of Physics, Melville, NY (2004), pp. 1635-1642.
4. Zagarola, M.V., Swift, W.L., Sixsmith, H., McCormick, J.A., and Izenson, M.G., "Development of a Turbo-Brayton Cooler for 6 K Space Applications," *Cryocoolers 12*, Kluwer Academic/Plenum Publishers, New York (2003), pp. 571-578.
5. NASA Goddard Space Flight Center, *General Environmental Verification Specification for STS and ELV Payloads, Subsystems, and Components*, GSFC Code 302, GEVS-SE, Rev A, Greenbelt, MD (June 1996).
6. Kroeger, P.G., "Performance Deterioration in High Effectiveness Heat Exchangers Due to Axial Heat Conduction Effects," *Advances in Cryogenic Eng.*, Vol. 31, Plenum Press, NY (1967), pp. 363-372.